Author Manuscript

Author Manuscript

Author Manuscript

Author Manuscript

HHS Public Access

Author manuscript

Neuron. Author manuscript; available in PMC 2016 August 19.

Published in final edited form as:

Neuron. 2015 August 19; 87(4): 840–852. doi:10.1016/j.neuron.2015.08.003.

Structured variability in Purkinje cell activity during locomotion

Britton A. Sauerbrei, **Evgueniy V. Lubenov**, and **Athanassios G. Siapas**

Computation and Neural Systems Program, Division of Biology and Biological Engineering, and Division of Engineering and Applied Science, California Institute of Technology, Pasadena, CA 91125

Athanassios G. Siapas: thanos@caltech.edu

Summary

The cerebellum is a prominent vertebrate brain structure that is critically involved in sensorimotor function. During locomotion, cerebellar Purkinje cells are rhythmically active, shaping descending signals and coordinating commands from higher brain areas with the step cycle. However, the variation in this activity across steps has not been studied, and its statistical structure, afferent mechanisms, and relationship to behavior remain unknown. Here, using multi-electrode recordings in freely moving rats, we show that behavioral variables systematically influence the shape of the step-locked firing rate. This effect depends strongly on the phase of the step cycle and reveals a functional clustering of Purkinje cells. Furthermore, we find a pronounced disassociation between patterns of variability driven by the parallel and climbing fibers. These results suggest that Purkinje cell activity not only represents step phase within each cycle, but is also shaped by behavior across steps, facilitating control of movement under dynamic conditions.

Introduction

Trial-to-trial variability is a widespread and fundamental feature of neural activity, evident from the periphery through higher brain areas. Responses to sensory stimuli vary over repeated presentations, and this variability is modulated by stimulus onset (Churchland et al., 2010; Monier et al., 2003), depends strongly on network architecture (Litwin-Kumar and Doiron, 2012), and is altered by successive stages of sensory processing (Kara et al., 2000). Furthermore, trial-to-trial correlations between neurons influence the accuracy of neural codes (Averbeck et al., 2006; Moreno-Bote et al., 2014), and are highly dependent on global changes in brain state (Ecker et al., 2014). During the preparation and execution of movement, neural activity often varies considerably across repetitions, even when the movement is highly stereotyped. Such variability is thought to impose critical constraints on motor performance (Shenoy et al., 2013; Todorov and Jordan, 2002), the capacity of motor

Publisher's Disclaimer: This is a PDF file of an unedited manuscript that has been accepted for publication. As a service to our customers we are providing this early version of the manuscript. The manuscript will undergo copyediting, typesetting, and review of the resulting proof before it is published in its final citable form. Please note that during the production process errors may be discovered which could affect the content, and all legal disclaimers that apply to the journal pertain.

Contributions

BAS and AGS designed the experiments. BAS performed the experiments. BAS, EVL, and AGS analyzed the data. BAS generated the figures. BAS, EVL, and AGS wrote the manuscript.

Author Manuscript Author Manuscript Author Manuscript Author Manuscript

codes (Averbeck and Lee, 2003; Lee et al., 1998; Maynard et al., 1999), and learning (Chaisanguanthum et al., 2014; Mandelblat-Cerf et al., 2009).

Several features make locomotion a powerful framework for studying neural variability in motor systems. First, locomotion is an ethologically relevant, nearly universal characteristic of animal life. Many aspects of legged overground movement are remarkably consistent across a wide range of species, from stick insects to humans (Orlovsky et al., 1999; Shik and Orlovsky, 1976), and the insights obtained from its study will likely generalize beyond the model organism chosen. Second, locomotion and other periodic behaviors are paradigmatic cases of motor repetition, with centrally generated rhythms shaped by modulatory influences. Third, studying locomotion eliminates the need for delays between experimental trials, allowing efficient acquisition of data from a large number of cycles and improving the statistical detection of patterns.

The cerebellum plays a critical role in the coordination of locomotion (Armstrong, 1988; Arshavsky et al., 1986; Shik and Orlovsky, 1976), and damage to the cerebellar vermis severely impairs the control of limbs and posture in animal models and in human patients (Dow and Moruzzi, 1958; Martino et al., 2014; Morton and Bastian, 2004). Furthermore, mouse mutant lines with cell-type-specific abnormalities in the cerebellar cortex exhibit locomotor deficits in speed, accuracy, consistency, and multi-joint coordination (Vinueza Veloz et al., 2014). During stepping, pathways from the spinal cord carry proprioceptive, cutaneous, and rhythmogenic signals to the cerebellar cortex (Arshavsky et al., 1986; Bosco and Poppele, 2001; Oscarsson, 1965). Mossy fibers related to the forelimbs, hindlimbs, and head have different distributions over cerebellar lobules but largely overlap (Adrian, 1943; Anderson, 1943; Dow and Moruzzi, 1958; Matsushita and Hosoya, 1979; Snyder et al., 1978; Tolbert and Gutting, 1997), and vestibular pathways terminate in the same areas (Barmack et al., 1992; Barmack et al., 1993; Denoth et al., 1979; Jensen, 1985; Kotchabhakdi and Walberg, 1978; Manzoni et al., 1999; Matsushita and Wang, 1987; Precht et al., 1977). Signals from these pathways are relayed through the parallel fibers to Purkinje cells in the vermal and intermediate cortex, which discharge periodically during stepping (Armstrong and Edgley, 1984, 1988; Edgley and Lidierth, 1988; Orlovsky, 1972; Udo et al., 1981) and impose their rhythm on routes descending back to the spinal cord (Arshavsky et al., 1986). This rhythmic discharge provides direct signals to the spinal limb controllers, and also gates motor commands from higher brain centers, ensuring that these commands are coordinated with the ongoing locomotor pattern (Orlovsky et al., 1999).

Although the cerebellar contribution to the control of locomotion has been studied extensively, a number of experimental challenges remain. Previous studies have used decerebrate (Arshavsky et al., 1986; Orlovsky, 1972; Udo et al., 1981) and awake (Armstrong and Edgley, 1984, 1988; Edgley and Lidierth, 1988) cats restricted on a treadmill, but none have examined step-locked simple and complex spikes in freely behaving rodents. Furthermore, treadmill studies of constant-speed stepping have dominated the study of cerebellar activity, but are limited in their ability to reveal the neuronal dynamics that occur in freely moving animals that spontaneously initiate, maintain, and terminate locomotion. Several studies have imaged calcium transients in Purkinje cell ensembles, revealing olivo-cerebellar interactions during locomotion (De Gruijl et al., 2014;

Author Manuscript Author Manuscript Author Manuscript Author Manuscript

Flusberg et al., 2008; Ghosh et al., 2011; Hoogland et al., 2015; Ozden et al., 2012). These transients, however, reflect complex spikes, which constitute only a small fraction of the spiking output. Few simultaneous recordings of simple spikes from multiple Purkinje cells have been made during locomotion (Smith, 1995), and correlations between pairs of neurons across steps have not been studied. Finally, Purkinje cell activity has been reported to vary extensively across steps (Armstrong and Edgley, 1984), but there has been no systematic study of this variation and its relationship to behavior, though some evidence suggests that animal speed can influence activity averaged over many steps (Armstrong and Edgley, 1988).

Here, we use chronically implanted multi-tetrode arrays in conjunction with electromyography and behavioral measurements in freely moving rats to address several open questions. First, is the step-locked firing pattern for a Purkinje cell highly stereotyped, or does it change extensively across steps? Furthermore, if this pattern is flexible, what are its major modes of variation? Second, how is neuronal variability related to behavior? Correlations between neuronal activity and behavioral factors would suggest that step-to-step variation plays a functional role in motor control, while the absence of correlations might indicate that such variation is noise. In addition, if such correlations are present, do they influence only the mean firing rate within a step cycle, or does interaction between behavior and spiking occur on a finer time scale through step-phase-dependent effects? Third, is the activity of multiple Purkinje cells correlated across steps? Uncorrelated activity would suggest that variation reflects intrinsic noise at the level of individual neurons, while pairwise correlations would be consistent with coordinated inputs. Fourth, how is Purkinje cell output shaped across steps by its two afferent systems, the parallel and climbing fibers? The contributions of these two pathways can be distinguished using extracellular recording: the parallel fibers control the rate of simple spikes, while the climbing fibers produce complex spikes (Eccles et al., 1966). One possibility is that both pathways use an analog rate code for sensorimotor variables both within steps (representing step phase) and across steps (representing behavioral factors such as speed). Alternatively, the two pathways might encode distinct features using qualitatively different coding schemes.

Results

Tetrode recordings from freely moving rats reveal high step-to-step variability

Using chronically implanted multi-tetrode arrays, we recorded spiking activity from 120 Purkinje cells in the medial cerebellar vermis of freely behaving rats (n=3; Figure 1A). Most cells were located in lobule V (n=74) and VI (n=42), with a small number in lobule IV (n=4) (Figure S3). All recorded neurons were identified as Purkinje cells by the presence of complex spiking (Eccles et al., 1966), and in many of these cells (n=65), it was possible to reliably distinguish between simple and complex spikes throughout the session (Figure 1B). The animals were trained to walk freely on a linear track for water reward at ports positioned at the ends of the track, while we recorded head location, head attitude, an EMG of acromiotrapezius activity, and the timing of licks at the water ports (Figure 1A, Figure S1). For most cells, firing rates were elevated during locomotion, relative to inactivity and licking (Figure S4C, $p < 10^{-7}$ and $p < 10^{-6}$, respectively, paired t-tests), and complex spikes

Author Manuscript Author Manuscript Author Manuscript Author Manuscript

also exhibited rate increases for the same states (Figure S4D, p = .0011 and p = .015, paired t-tests). Phasic increases in firing occurred at the onset of locomotion, and phasic increases or decreases were common during movement termination (Figure S4A). Lick times were recorded for 114 cells, and 101 of these were significantly modulated by licking (Figure S4B, Kuiper's test, false discovery rate set at q = .05).

All cells discharged rhythmically during locomotion (Figure 1C, Figure 2A, B; q = .05, Kuiper's test), consistent with previous studies of paravermal lobule V in awake cats on a treadmill (Armstrong and Edgley, 1984, 1988; Edgley and Lidierth, 1988). Cells exhibited one (n=26), two (n=69), or three (n=25) peaks in the step cycle, and the location of these peaks was widely dispersed across cells (Figure 2B). However, although the average activity of each cell exhibited clear tuning to step phase, an inspection of spiking patterns across individual steps revealed a high degree of variability. The firing rate of the Purkinje cell in Figure 1C, for instance, shows large fluctuations within each step cycle, but even more striking are the changes in its amplitude and shape across steps. This extensive step-to-step variability was typically observable in the step-locked spike rasters (Figure 2A, **lower panel**) and firing rate curves (Figure 2C).

In order to quantify this variability, we computed the variance-to-mean ratio, or Fano factor, for the spike counts within a window starting at the EMG peak for each step cycle (Figure 2D, above). For a Poisson process, the count variance equals the count mean, and the Fano factor is one. By contrast, Purkinje cell spike counts typically had higher variances than means (Figure 2E, left panel), with a mean Fano Factor of 1.58 for a window duration of 350ms. These values indicate that spiking is more variable than expected for a Poisson process, and more variable than previously reported for macaque neocortical neurons during visually-guided reaching (e.g. supplementary motor area (Averbeck and Lee, 2003; Mandelblat-Cerf et al., 2009), motor cortex (Mandelblat-Cerf et al., 2009), premotor cortex (Churchland et al., 2010; Churchland et al., 2006), and the parietal reach region (Churchland et al., 2010)). Interestingly, we observed a strong disassociation between patterns of variability for simple spikes, which were over-dispersed relative to a Poisson process, and for complex spikes, which were under-dispersed (Figure 2D, below, 2E, center and right).

Patterns of variability in step-locked firing rates

If firing patterns differ across steps, what are the major modes of variation? In order to address this question, we performed principal component analysis on the step-locked firing rates for each cell. This produced an effective reduction of the data, with the first three components accounting for an average of 75% of the variance (Figure 3B, **left**). Sorting cycles by principal component scores (Figure S5) or visualizing the effects of the coefficients as perturbations of the mean firing rate curve (Figure 3A) revealed several common patterns: "bias" (an additive shift in the curve with little change in its shape), "amplitude" (multiplicative scaling of the curve), and "phase" (a horizontal shift of the curve forward or backward in time). These same three patterns have been independently identified in kinematic data from humans during locomotion (Ramsay and Silverman, 2005). While many cells had components that directly reflected one of these modes, more complex patterns were observed, as well. For instance, some cells with multiple peaks exhibited

Author Manuscript Author Manuscript Author Manuscript Author Manuscript

components that shifted the firing rate around one of the peaks, while imposing little change on the rest of the curve (e.g. component 1 for the cell marked with red arrow in Figure 3A, corresponding to the neuron from Figure 1C).

To quantify the extent to which a component represented a change in bias, amplitude, or phase, we computed three scores corresponding to these patterns: S_{bias}, S_{amp}, and S_{phase} (see methods section). Across the sample of Purkinje cells, the first principal component had much higher bias scores than the second ($p < 10^{-9}$, Kolmogorov-Smirnov test) and third ($p < 10^{-23}$) components (Figure 3B), and the second component had higher bias scores than the third ($p < 10^{-4}$), indicating that differences across steps were due largely to shifts in the mean firing rate. By contrast, the phase shift scores were much lower for the first principal component than for the second ($p < 10^{-6}$) and third ($p < 10^{-11}$), and for the second than the third ($p = .0023$). Furthermore, three-dimensional scatterplots revealed an aggregation of neurons around a pure bias shift for the first component, and around a pure phase shift for the third component (Figure 3C).

Neural variability exhibits step-phase-dependent correlations with behavior

Are these step-to-step fluctuations in neuronal spiking related to behavior? Examination of the spiking activity of individual neurons over several laps often suggested systematic changes in step-locked firing rates with behavioral variables, such as speed (Figure 4A). In order to characterize this further, we first measured the animals' average head speed, acceleration, roll, pitch, and EMG amplitude within each step and examined their relationship to the firing rates. For each neuron and behavioral variable, we divided the steps into intervals according to the value of the variable and averaged the firing rate curves within each interval (see methods section). This often produced a sequence of curves that varied smoothly and systematically as the behavioral parameters changed (Figure 4B, C). In order to quantify the effects of behavior on neuronal activity, we estimated a linear model for each Purkinje cell, with speed, acceleration, roll, pitch, and EMG amplitude as independent variables and the mean firing rate on each cycle as the dependent variable. Speed, acceleration, and head attitude had significant effects for many cells. Out of 120 total Purkinje cells, 81 were modulated by speed, 84 by acceleration, 70 by roll, and 54 by pitch (Figure S6A). By contrast, only 27 neurons were significantly modulated by EMG amplitude. For each independent variable, both positive and negative regression coefficients were observed, but most significant values were positive for speed ($p = .014$, binomial test). An examination of coefficients for pairs of variables failed to reveal any clustering of Purkinje cell tuning properties: instead, a broad distribution of values was observed (Figure S6B).

If behavior is correlated with Purkinje cell activity, what is the structure of its relationship to the step-phase-dependent firing rate? This question is central, for two reasons. First, cycle-to-cycle variability is not restricted to shifts in mean firing rate, but can express a variety of patterns, as indicated by the analysis of principal component coefficients (Figure 3). Second, the behavioral variables – particularly roll, pitch, and EMG amplitude – can fluctuate on a faster time scale than that of a single step cycle (Figure S1). In order to address this question, we estimated regression curves parameterized by step phase for each cell and

Author Manuscript Author Manuscript Author Manuscript Author Manuscript

behavioral variable. These curves capture how a given behavioral variable modulates the shape of the step-locked firing rate for each cell. For many cells, the relationship between behavior and neural activity varied in magnitude, and in some cases in sign, according to the phase of the step cycle (Figure 4D). For example, the neuron on the left in Figure 4D shows a decrease with speed during the first half of the step cycle, but an increase with speed during the second half. Consequently, this neuron's speed regression curve has a shape similar to its average firing rate curve, and imposes a strong amplitude shift. To further quantify the patterns of this behavioral modulation, we computed bias, amplitude, and phase scores for these curves (see Supplemental Experimental Procedures). Three-dimensional scatterplots of scores (S_{bias}, S_{amp}, and S_{phase}) for the regression curves revealed large differences between behavioral variables, as well as the presence of clusters (Figure 4E). We performed a hierarchical cluster analysis on the (S_{bias}, S_{amp}, S_{phase}) observations for cells with significant tuning to each variable, and this analysis revealed several key features. First, all variables except EMG amplitude exhibited a large aggregation of cells around a pure bias shift. Second, speed and pitch exhibited clusters near a pure amplitude shift. Third, roll and acceleration exhibited clusters near a pure phase shift. These results demonstrate a functional segregation in Purkinje cell properties that is not observed after averaging behavior and firing rates within each step cycle.

Purkinje cell pairs exhibit correlated activity across steps

In many sessions, it was possible to record simultaneously from multiple Purkinje cells, and step-averaged firing rates for pairs often appeared to covary across steps (Figure 5A). Such covariation may result in part from similar tuning to measured behavioral variables, so we first removed the effects of these factors using the regression models and then examined correlations between the residuals. Scatterplots of the residual firing rates for pairs recorded on distinct tetrodes revealed clear associations in many cases (Figure 5B, above), and 40 out of 89 pairs were significantly correlated (Figure 5B, below; q = .05, partial rank correlation), with both positive and negative correlations observed. Further analysis of the residuals and the rank-transformed variables indicated that the correlations were unlikely to be due to nonlinear interactions between measured behavioral variables and firing rates (Figure S7). These correlations suggest that step-to-step variability is not independent, intrinsic noise at the level of individual Purkinje cells, but is rather driven by coordinated inputs. The relative spatial location of recorded cells did not influence correlations: no significant differences were observed between ipsilateral and contralateral pairs (p = .27, two-sample t-test), between cells in the same lobule and in different lobules (p = .35, two-sample t-test), or between cells at different mediolateral or rostrocaudal distances (p = .95, .92, respectively, one-way ANOVA) (Figure 5C).

Parallel and climbing fiber inputs carry qualitatively distinct signals

Because the climbing fiber system plays an essential role in motor performance and learning, we examined the relationship between complex spikes, which are driven by this pathway, and step phase, speed, acceleration, head posture, and EMG. In contrast to simple spikes, which were strongly modulated by the stepping rhythm for all Purkinje cells, complex spikes were modulated in a minority of neurons (12/65; q = .05, Kuiper's test; Figure 6A, B). The depth of modulation was larger for simple than complex spikes (p <

Author Manuscript Author Manuscript Author Manuscript Author Manuscript

10^{-9}, paired t-test), though high values were occasionally observed for complex spikes (Figure 6B, left). Most of these observations, however, were from datasets with relatively few steps (Figure 6B, right), and did not achieve statistical significance, suggesting that some large deviations from uniformity might have been artifacts of small sample size. Furthermore, the estimation of linear models for step-locked spike counts failed to reveal effects of speed, acceleration, roll, pitch, and EMG amplitude: no regression coefficients differed significantly from zero (q = .05, Figure 6C). Thus, our data suggest that while simple spikes are strongly related to locomotor behavior within steps (through step phase) and across steps (through speed, acceleration, and head posture), complex spikes show only modest tuning to step phase, and no tuning to behavioral variables across steps.

Purkinje cell properties differ across cerebellar lobules

Although the mossy fiber pathways into cerebellar lobule V and into lobule VI overlap extensively, they differ in their density, anatomical origin, and function. For instance, proprioceptive and cutaneous pathways from the forelimbs terminate more extensively in lobule V, whereas inputs from the head and neck are more prominent in lobule VI (Adrian, 1943; Anderson, 1943; Barmack et al., 1992; Barmack et al., 1993; Dow and Moruzzi, 1958; Kotchabhakdi and Walberg, 1978; Matsushita and Hosoya, 1979; Snyder et al., 1978; Tolbert and Gutting, 1997). We therefore explored potential differences between our samples of lobule V and lobule VI Purkinje cells. Although cells in both regions were tuned to the stepping rhythm and exhibited speed-, acceleration-, and head posture-related variation across steps, several differences between lobules emerged. In lobule VI, mean firing rates were higher (Figure 7B, $p < 10^{-4}$), and there was a stronger relationship between head posture and step-locked activity (p = .012), while lobule V cells were more strongly modulated by acceleration (p = .0011). Although we observed lobular differences in the distributions of several features, these distributions were largely overlapping, and did not result in a clear separation of lobule V and VI neurons (Figure 7C). Furthermore, a higher fraction of cells had multiple peaks in the step cycle for lobule V than lobule VI (Figure 7A; 91% vs 55%, $p < 10^{-4}$, Fisher's exact test). These differences are consistent with a functional segregation in the vermis during locomotion, with lobule V playing a greater role in limb control and lobule VI acting to maintain postural stability of the head.

Discussion

The data obtained and analyzed here represent, to our knowledge, the first recordings of simple and complex spikes from cerebellar Purkinje cells in freely moving rodents during stepping, as well as the first study of step-to-step fluctuations in these cells in any species. While natural movement is expected to produce variable neural responses, we wish to emphasize not the absolute magnitude of variability, but its rich statistical structure, which reveals several key insights. First, the variability expresses characteristic bias, amplitude, and phase motifs, which are consistent with the encoding of kinematic variables. Second, this variability is related to multiple movement parameters in a step-phase-dependent way. Third, an analysis of the phase-dependent regression curves reveals functional clusters of Purkinje cells: for instance, one group of cells is amplitude-modulated by speed, while another is phase-modulated by head roll. Fourth, the presence of step-to-step correlations for

Author Manuscript Author Manuscript Author Manuscript Author Manuscript

many pairs of cells, as well as correlations between behavior and spiking, suggest variability is not mainly due to intrinsic, single-neuron noise. Finally, there is a pronounced disassociation between patterns of variability driven by the parallel and climbing fiber systems, suggesting that they use qualitatively distinct coding schemes.

One limitation of our chronic, freely moving preparation is that it does not allow direct assessment of proprioceptive, vestibular, and somatosensory properties of neurons, which must be measured under much more controlled conditions (typically, head fixation and anesthesia). Furthermore, optical measurements of multi-joint kinematics are highly challenging in small animals freely navigating an environment. Thus, while we can establish a correspondence between neuronal activity and measured variables such as speed and head attitude, it is difficult to establish whether these are the primary variables encoded, or are simply correlated with other variables that drive the responses. However, in contrast with head fixed and treadmill-based designs, our approach allows a direct measurement of neuronal activity during the natural initiation, modulation, and termination of locomotion, and reveals much richer statistical structure in this activity than previously demonstrated.

Several factors could be responsible for the observed variability across steps. If Purkinje cells encoded kinematic variables such as joint angle, the neural variability might reflect variability in kinematics. For instance, at higher speeds of locomotion, joint angle excursions tend to be larger (Costa et al., 2010), and neural signals encoding angle should have larger amplitudes at higher speeds. Indeed, the strong amplitude modulation by speed observed for many cells (Figure 4C, D, E) is consistent with this hypothesis. Alternatively, the step-to-step variability could reflect variation in external forces (Bernstein, 1967). In order to maintain a periodic movement trajectory, the nervous system must compute the difference between the desired periodic force profile and perturbations due to ground reaction forces, gravity, and other external sources. These external perturbations may be aperiodic and highly variable, and might consequently produce a neural difference signal that is much more variable than the movement itself. Our observation of step-locked firing profiles that varied considerably, even for consecutive steps (Figure 1C, 2A), might result in part from the participation of Purkinje cells in this computation.

The behavior-dependent modification of the step-locked firing pattern likely enhances motor performance both directly, through feedforward routes to the spinal cord, and indirectly, by gating neocortical commands. The direct, feedforward pathways provide speed- and posture-dependent modification of motor parameters, such as the amplitude, duty cycle, and timing of muscle activity, while leaving the basic stepping rhythm intact. On the other hand, the indirect, gating pathway could coordinate cortically-initiated commands with locomotion, as when a walking animal needs to brake suddenly in response to a visual stimulus, correct a postural disturbance, or step over an obstacle. In order to execute these movements effectively, the descending control signals must meet two criteria. First, they must have an amplitude that scales with the animal’s speed or posture across steps; for instance, at higher speeds, a larger braking signal is required to generate larger extensor forces and stop the animal. Second, they must be appropriately timed within the step cycle; a braking command that increases extensor activity during swing will likely cause the animal to stumble. These two criteria could be satisfied through a multiplicative interaction between a binary

Author Manuscript Author Manuscript Author Manuscript Author Manuscript

neocortical command and a cerebellar gating signal that depended on both step phase and speed. The resulting output would scale with the animal's speed, producing larger braking forces when the animal moved faster. Crucially, it would also vary with step phase within each cycle, allowing braking to be initiated only during the correct part of the cycle. Thus, a cortical signal with a fixed amplitude initiated at an arbitrary speed and step phase would produce a descending control signal with the appropriate amplitude and timing.

Previous work in cats performing treadmill locomotion at two discrete speeds has demonstrated that step-averaged Purkinje cell firing rates tend to be higher at faster speeds (Armstrong and Edgley, 1988). Our results advance this work in four key respects. First, our use of continuous, natural variation in behavior over a wide range rather than at two discrete points allows us to precisely estimate the magnitude of behavioral effects on firing rate (Figure S6A). Second, our simultaneous measurement of several behavioral variables enables us to model the joint effects of these variables in the same cells (Figure S6B). Third, our estimation of phase-dependent regression curves demonstrates that behavioral variables do not merely produce changes in mean firing rate, but may also have effects that depend strongly on step phase (Figure 4D). Finally, our analysis of bias, amplitude, and phase scores for these regression curves reveals that the Purkinje cell population is not uniform, but highly heterogeneous, and exhibits functional clusters (Figure 4E). For instance, speed and pitch tend to influence either the bias or the amplitude of the firing rate curve, while acceleration and roll may modulate the phase. These results depend critically on our analysis of variability both across steps and within the step cycle, and would be obscured by averaging over either.

Our findings show that the parallel and climbing fiber systems convey different types of information to Purkinje cells during locomotion: simple spikes are modulated both within the step cycle (by step phase) and across steps (by speed and head posture), while complex spikes show only moderate tuning within the step cycle, and no effect of behavioral variables across steps. In addition, the low Fano factors observed for complex spikes suggest that behavioral fluctuations during movement do not imply that neural responses will be variable throughout the motor system. These findings are consistent with the idea that the climbing fiber system conveys a sparse, impulse-like signal that shapes parallel fiber synaptic weights, but does not use an analog rate code for sensorimotor variables (Albus, 1971; Marr, 1969). However, because our experimental approach does not permit high-density sampling of complex spikes from Purkinje cells within the same microzone, our results do not rule out the possibility that locomotor parameters are encoded through complex spike synchrony, rather than rates. Indeed, recent calcium imaging studies have demonstrated that correlated complex spike activity increases significantly during locomotion relative to rest, particularly around movement onset (De Gruijl et al., 2014; Ozden et al., 2012), but that this increase does not occur in mice lacking connexin36, which is essential for gap junction coupling of olivary ensembles (De Gruijl et al., 2014). Furthermore, mice with P/Q-type calcium channel abnormalities exhibit a lack of microzonal complex spike synchrony and pronounced deficits in timing, accuracy, and interlimb coordination during stepping (Hoogland et al., 2015).

Author Manuscript Author Manuscript Author Manuscript Author Manuscript

Although complex spikes were tuned to step phase for only a minority (12/65) of Purkinje cells, this result contrasts with previous work in the paravermis (Armstrong et al., 1988) and lateral vermis (Andersson and Armstrong, 1987) of awake, intact cats, which did not reveal statistically significant complex spike modulation during stepping. This discrepancy might be due to our analysis of a larger number of steps (mean of 1064 cycles, compared with approximately 100 cycles), or to our choice of statistical technique (a test based on the circular empirical distribution function, compared with a test based on histogram extrema). The difference might also be due to the location of the recorded cells, which were more medial in our sample, or to our use of rats as experimental animals, instead of cats.

We observed large correlations between many pairs of simultaneously-recorded Purkinje cells, providing further evidence that step-to-step variability does not merely reflect intrinsic noise at the level of individual neurons, but is rather a result of coordinated inputs (Lee et al., 1998). These correlations are not simply due to similar tuning to speed, acceleration, and head posture, since they persist after removing the effects of these factors. Furthermore, the prevalence of both positive and negative partial correlations suggests that the coordination is not merely shared drive from the central pattern generator or from a single muscle or joint, but rather reflects cells' different weightings of a range of inputs. As previous studies in cerebral cortex have suggested (Averbeck and Lee, 2003; Lee et al., 1998; Maynard et al., 1999), the presence of correlations in ensemble activity might constrain the encoding of movement parameters.

Several overlapping pathways into lobules V and VI of the vermis are likely responsible for the influence of step phase, speed, acceleration, and head attitude on Purkinje cell activity. Proprioceptive and cutaneous information from the forelimbs and hindlimbs arrives through spinocerebellar and cuneocerebellar tracts (Adrian, 1943; Anderson, 1943; Matsushita and Hosoya, 1979; Snyder et al., 1978; Tolbert and Gutting, 1997), some of which also carry signals from the spinal rhythm generating network (Arshavsky et al., 1986). Information about head posture arrives through primary (Barmack et al., 1993) and secondary (Barmack et al., 1992; Kotchabhakdi and Walberg, 1978; Matsushita and Wang, 1987) vestibular projections and through the central cervical nucleus (Matsushita and Hosoya, 1979; Snyder et al., 1978), which receives both vestibular and neck proprioceptive signals (Popova et al., 1995; Thomson et al., 1996). The convergence of vestibular and proprioceptive pathways in the dorsal vermis is consistent with physiological studies (Jensen, 1985; Precht et al., 1977), which have identified individual Purkinje cells responsive to both neck and vestibular stimulation (Denoth et al., 1979; Manzoni et al., 1999). The modulation of Purkinje cell activity both within and across steps, then, likely reflects the integration of signals from diverse pathways and modalities.

Although Purkinje cells in both lobule V and lobule VI are modulated by step phase, speed, acceleration, and head posture, our data do provide evidence for functional differences between lobules. Cells in lobule V were more strongly influenced by acceleration and had multiple firing peaks in the step cycle, suggesting that they might control the activity of multiple joints, or of single joints undergoing multiple cycles of flexion and extension per step. Cells in lobule VI, on the other hand, were more strongly modulated by head posture

Author Manuscript Author Manuscript Author Manuscript Author Manuscript

than lobule V cells, suggesting that they help maintain the stability of the head during stepping.

Taken together, these results reveal several novel features of Purkinje cell activity during locomotion that would not have been apparent after averaging. The strategy of averaging within steps to obtain a scalar firing rate for each cycle (Figure 8B) has the advantage of revealing the relationship between behavioral variables and neuronal activity, but obscures the functionally critical (Arshavsky et al., 1986) and often complex dependence of activity on step phase. On the other hand, averaging across steps to obtain the phase-dependent firing rate (Figure 8C) obscures the extent and statistical structure of step-to-step variability, as well as step-to-step correlations between behavior and Purkinje cell activity, and between the firing rates of multiple neurons. Our findings suggest a dynamic view of neuronal activity during locomotion, in which a step-phase-dependent firing pattern is itself modulated by behavior during ongoing movement (Figure 8D).

Experimental Procedures

Task and behavioral measurements

Three male Long-Evans rats were trained to walk for water reward on a 1.8m-long linear track (Figure 1A). Animal position was measured using three headstage-mounted LEDs and an overhead camera. Head pitch and roll were estimated using a head-mounted inertial measurement unit. The stepping rhythm was identified by detecting sequences of peaks in the acromiotrapezius EMG (see Supplemental Experimental Procedures, Figure S2). The step phase was obtained by linear interpolation, with the EMG peak defined as 0 for cells ipsilateral to the muscle and on the midline, and as π for contralateral cells.

Electrophysiology

Rats were chronically implanted with twenty independently adjustable tetrodes targeted to lobules V and VI of the cerebellar vermis, spanning +/− 1mm of the midline (Figure S3). Signals were buffered on the headstage, amplified, and acquired as 24-bit samples at 25kHz. Spikes were clustered by fitting a mixture model in a 12-dimensional feature space, using 3 waveform principal components per tetrode channel (Calabrese and Paninski, 2011; Ecker et al., 2014; Tolias et al., 2007). For cells with large and stable complex spikes, a second stage of clustering was performed on the raw waveforms within −2/+10 ms of each spike to distinguish simple from complex spikes. For analyses that did not compare simple and complex spike activity, the cell's spike train was taken to be the union of spikes of both types. At the end of each experiment, electrolytic lesions were applied at each recording site, and the tetrode locations were verified in Hoescht-stained tissue sections (Figure S3).

Statistical analysis

The state-dependent mean firing rates for locomotion, licking, and inactivity were defined as the total number of spikes occurring in the state divided by the total duration of the state throughout the dataset. For each Purkinje cell, a circular distribution was fit to the step phases sampled at the spike times. To determine whether spiking was locked to the step cycle, Kuiper's test was used (Mardia and Jupp, 2000) for both simple and complex spikes.

Author Manuscript Author Manuscript Author Manuscript Author Manuscript

The step-to-step variability of spike counts was quantified using the variance-to-mean ratio, or Fano factor (Figure 2D), computed for spike counts within windows starting at each EMG peak.

In order to study the shape of step-locked firing rate curves, the spike trains were smoothed with a 25ms Gaussian kernel, and the curves were extracted for each step, with the time axis normalized so that each curve was parameterized by step phase θ, rather than time. Principal component analysis was performed on the curves for each cell, and the effect of each component, $w(\theta)$, was visualized as a perturbation of the mean curve, $f(\theta)$ (Ramsay and Silverman, 2005). The extent to which each component was an additive shift, a multiplicative scaling, or a phase shift was determined by computing bias, amplitude, and phase scores, respectively (see supplemental experimental procedures).

The influence of behavioral variables on Purkinje cell activity across steps was first determined by averaging speed, forward acceleration, sin(roll), and sin(pitch), and EMG amplitude within each step cycle. To study the variation in curve shape with behavior, slicing intervals for behavioral values were determined using an equal-count algorithm with twelve (Figure 4B) or six (Figure 4C) intervals and 50% overlap (Cleveland, 1993). Step-locked firing rates were then averaged within each interval.

In order to quantify the influence of behavior on spiking, we defined the firing rate on each step to be the number of spikes occurring during that step divided by the step duration. We converted the firing rate and the behavioral variables to z-scores, and estimated a multiple regression model for each cell. In order to study how the relationship between neural activity and behavior varies throughout the step cycle, we next estimated step-phase-dependent regression curves (Figure 4D) and computed bias, amplitude, and phase scores for these curves (see Supplemental Experimental Procedures). For each behavioral variable, we performed a cluster analysis of these bias, amplitude, and phase triplets (Figure 4E). The low rate of complex spikes did not permit the analysis of step-locked firing rates; instead, we studied the effects of behavioral variables on the number of complex spikes, within a 350ms window starting at the onset of each step cycle. For each Purkinje cell with stable complex spikes, we estimated a Poisson regression model.

Coordinated activity between pairs of cells was assessed using the partial rank correlations in the step-averaged firing rates: the effects of the behavioral variables were first removed using the multiple regression model, and Spearman's ρ was computed between the residuals. For the analysis of step phase modulation, the linear models, and the pairwise correlations, corrections for multiple comparisons were made by setting the false discovery rate to $q = .05$ (Benjamini and Hochberg, 1995).

Supplementary Material

Refer to Web version on PubMed Central for supplementary material.

Author Manuscript Author Manuscript Author Manuscript Author Manuscript

Acknowledgements

We thank Michael Dickinson, Gilles Laurent, and Andreas Tolias for comments on the manuscript, Maria Papadopoulou for advice on histology, Kevin Shan for development of the inertial measurement unit, and the members of the Siapas lab for valuable discussions. This work was supported by the Moore Foundation, the Mathers Foundation, NIH DP1OD008255, and NSF 1146871.

References

Adrian E. Afferent Areas in the Cerebellum Connected with the Limbs. Brain. 1943; 66:289–315.

Albus J. A theory of cerebellar function. Mathematical Biosciences. 1971; 10:25–61.

Anderson RF. Cerebellar Distribution of the Dorsal and Ventral Spino-Cerebellar Tracts in the White Rat. The Journal of Comparative Neurology. 1943; 79:415–423.

Andersson G, Armstrong DM. Complex spikes in Purkinje cells in the lateral vermis (b zone) of the cat cerebellum during locomotion. The Journal of physiology. 1987:107–134. [PubMed: 3656160]

Armstrong DM. The supraspinal control of mammalian locomotion. The Journal of Physiology. 1988; 405:1–37. [PubMed: 3076600]

Armstrong DM, Edgley SA. Discharges of Purkinje cells in the paravermal part of the cerebellar anterior lobe during locomotion. The Journal of physiology. 1984:403–424. [PubMed: 6747896]

Armstrong DM, Edgley SA. Discharges of interpositus and Purkinje cells of the cat cerebellum during locomotion under different conditions. The Journal of physiology. 1988; 400:425–445. [PubMed: 3418533]

Armstrong DM, Edgley SA, Lidierth M. Complex spikes in Purkinje cells of the paravermal part of the anterior lobe of the cat cerebellum during locomotion. The Journal of Physiology. 1988:405–414. [PubMed: 3418531]

Arshavsky, YI.; Gelfand, IM.; Orlovsky, GN. Cerebellum and rhythmical movements. Berlin ; New York: Springer-Verlag; 1986.

Averbeck BB, Latham PE, Pouget A. Neural correlations, population coding and computation. Nature Reviews Neuroscience. 2006; 7:358–366. [PubMed: 16760916]

Averbeck BB, Lee D. Neural noise and movement-related codes in the macaque supplementary motor area. J Neurosci. 2003; 23:7630–7641. [PubMed: 12930802]

Barmack NH, Baughman RW, Eckenstein FP, Shojaku H. Secondary vestibular cholinergic projection to the cerebellum of rabbit and rat as revealed by choline acetyltransferase immunohistochemistry, retrograde and orthograde tracers. J Comp Neurol. 1992; 317:250–270. [PubMed: 1577999]

Barmack NH, Baughman RW, Errico P, Shojaku H. Vestibular primary afferent projection to the cerebellum of the rabbit. J Comp Neurol. 1993; 327:521–534. [PubMed: 7680050]

Benjamini Y, Hochberg Y. Controlling the False Discovery Rate - a Practical and Powerful Approach to Multiple Testing. J Roy Stat Soc B Met. 1995; 57:289–300.

Bernstein, NA. The co-ordination and regulation of movements. 1st English edn. Oxford, New York: Pergamon Press; 1967.

Bosco G, Poppele RE. Proprioception from a spinocerebellar perspective. Physiological reviews. 2001; 81:539–568. [PubMed: 11274339]

Calabrese A, Paninski L. Kalman filter mixture model for spike sorting of non-stationary data. J Neurosci Methods. 2011; 196:159–169. [PubMed: 21182868]

Chaisanguanthum KS, Shen HH, Sabes PN. Motor variability arises from a slow random walk in neural state. J Neurosci. 2014; 34:12071–12080. [PubMed: 25186752]

Churchland MM, Yu BM, Cunningham JP, Sugrue LP, Cohen MR, Corrado GS, Newsome WT, Clark AM, Hosseini P, Scott BB, et al. Stimulus onset quenches neural variability: a widespread cortical phenomenon. Nat Neurosci. 2010; 13:369–378. [PubMed: 20173745]

Churchland MM, Yu BM, Ryu SI, Santhanam G, Shenoy KV. Neural variability in premotor cortex provides a signature of motor preparation. J Neurosci. 2006; 26:3697–3712. [PubMed: 16597724]

Cleveland, WS. Visualizing data. Murray Hill, N.J.: AT&T Bell Laboratories; 1993.

Author Manuscript Author Manuscript Author Manuscript Author Manuscript

Costa LM, Pereira JE, Filipe VM, Couto PA, Magalhaes LG, Bulas-Cruz J, Mauricio AC, Geuna S, Varejao AS. The effect of gait speed on three-dimensional analysis of hindlimb kinematics during treadmill locomotion in rats. Reviews in the neurosciences. 2010; 21:487–497. [PubMed: 21438195]

De Gruijl JR, Hoogland TM, De Zeeuw CI. Behavioral correlates of complex spike synchrony in cerebellar microzones. J Neurosci. 2014; 34:8937–8947. [PubMed: 24990915]

Denoth F, Magherini PC, Pompeiano O, Stanojevic M. Responses of Purkinje cells of the cerebellar vermis to neck and macular vestibular inputs. Pflugers Archiv : European journal of physiology. 1979; 381:87–98. [PubMed: 41218]

Dow, RS.; Moruzzi, G. The physiology and pathology of the cerebellum. Minneapolis: University of Minnesota Press; 1958.

Eccles JC, Llinas R, Sasaki K. The excitatory synaptic action of climbing fibers on the Purkinje cells of the cerebellum. The Journal of Physiology. 1966; 182:268–296. [PubMed: 5944665]

Ecker AS, Berens P, Cotton RJ, Subramaniyan M, Denfield GH, Cadwell CR, Smirnakis SM, Bethge M, Tolias AS. State Dependence of Noise Correlations in Macaque Primary Visual Cortex. Neuron. 2014; 82:235–248. [PubMed: 24698278]

Edgley SA, Lidierth M. Step-Related Discharges of Purkinje-Cells in the Paravermal Cortex of the Cerebellar Anterior Lobe in the Cat. The Journal of Physiology. 1988; 401:399–415. [PubMed: 3171993]

Flusberg BA, Nimmerjahn A, Cocker ED, Mukamel EA, Barretto RP, Ko TH, Burns LD, Jung JC, Schnitzer MJ. High-speed, miniaturized fluorescence microscopy in freely moving mice. Nat Methods. 2008; 5:935–938. [PubMed: 18836457]

Ghosh KK, Burns LD, Cocker ED, Nimmerjahn A, Ziv Y, El Gamal A, Schnitzer MJ. Miniaturized integration of a fluorescence microscope. Nat Methods. 2011; 8:871-U147. [PubMed: 21909102]

Hoogland TM, De Gruijl JR, Witter L, Canto CB, De Zeeuw CI. Role of Synchronous Activation of Cerebellar Purkinje Cell Ensembles in Multi-joint Movement Control. Current biology : CB. 2015; 25:1157–1165. [PubMed: 25843032]

Jensen DW. Posture-correlated responses to vestibular polarization in vermal versus intermediate posterior cerebellar cortex. Exp Neurol. 1985; 88:629–639. [PubMed: 3873351]

Kara P, Reinagel P, Reid RC. Low response variability in simultaneously recorded retinal, thalamic, and cortical neurons. Neuron. 2000; 27:635–646. [PubMed: 11055444]

Kotchabhakdi N, Walberg F. Cerebellar afferent projections from the vestibular nuclei in the cat: an experimental study with the method of retrograde axonal transport of horseradish peroxidase. Exp Brain Res. 1978; 31:591–604. [PubMed: 350598]

Lee D, Port NL, Kruse W, Georgopoulos AP. Variability and correlated noise in the discharge of neurons in motor and parietal areas of the primate cortex. J Neurosci. 1998; 18:1161–1170. [PubMed: 9437036]

Litwin-Kumar A, Doiron B. Slow dynamics and high variability in balanced cortical networks with clustered connections. Nat Neurosci. 2012; 15:1498–1505. [PubMed: 23001062]

Mandelblat-Cerf Y, Paz R, Vaadia E. Trial-to-trial variability of single cells in motor cortices is dynamically modified during visuomotor adaptation. J Neurosci. 2009; 29:15053–15062. [PubMed: 19955356]

Manzoni D, Pompeiano O, Bruschini L, Andre P. Neck input modifies the reference frame for coding labyrinthine signals in the cerebellar vermis: a cellular analysis. Neuroscience. 1999; 93:1095–1107. [PubMed: 10473274]

Mardia, KV.; Jupp, PE. Directional statistics. New York: J. Wiley; 2000.

Marr D. A theory of cerebellar cortex. The Journal of Physiology. 1969; 202:437–470. [PubMed: 5784296]

Martino G, Ivanenko YP, Serrao M, Ranavolo A, d'Avella A, Draicchio F, Conte C, Casali C, Lacquaniti F. Locomotor patterns in cerebellar ataxia. J Neurophysiol. 2014; 112:2810–2821. [PubMed: 25185815]

Matsushita M, Hosoya Y. Cells of origin of the spinocerebellar tract in the rat, studied with the method of retrograde transport of horseradish peroxidase. Brain Research. 1979; 173:185–200. [PubMed: 90539]

Author Manuscript Author Manuscript Author Manuscript Author Manuscript

Matsushita M, Wang CL. Projection pattern of vestibulocerebellar fibers in the anterior vermis of the cat: an anterograde wheat germ agglutinin-horseradish peroxidase study. Neurosci Lett. 1987; 74:25–30. [PubMed: 2436104]

Maynard EM, Hatsopoulos NG, Ojakangas CL, Acuna BD, Sanes JN, Normann RA, Donoghue JP. Neuronal interactions improve cortical population coding of movement direction. J Neurosci. 1999; 19:8083–8093. [PubMed: 10479708]

Monier C, Chavane F, Baudot P, Graham LJ, Fregnac Y. Orientation and direction selectivity of synaptic inputs in visual cortical neurons: a diversity of combinations produces spike tuning. Neuron. 2003; 37:663–680. [PubMed: 12597863]

Moreno-Bote R, Beck J, Kanitscheider I, Pitkow X, Latham P, Pouget A. Information-limiting correlations. Nat Neurosci. 2014; 17:1410–1417. [PubMed: 25195105]

Morton SM, Bastian AJ. Cerebellar control of balance and locomotion. The Neuroscientist. 2004; 10:247–259. [PubMed: 15155063]

Orlovsky GN. Activity of the Purkinje cells during locomotion. Biofizika. 1972; 5:891–896.

Orlovsky, GN.; Deliagina, TG.; Grillner, S. Neuronal control of locomotion : from mollusc to man. New York: Oxford University Press; 1999.

Oscarsson O. Functional Organization of the Spino- and Cuneocerebellar Tracts. Physiological Reviews. 1965; 45:495–522. [PubMed: 14337566]

Ozden I, Dombeck Da, Hoogland TM, Tank DW, Wang SS-H. Widespread state-dependent shifts in cerebellar activity in locomoting mice. PloS one. 2012; 7:e42650. [PubMed: 22880068]

Popova LB, Ragnarson B, Orlovsky GN, Grant G. Responses of neurons in the central cervical nucleus of the rat to proprioceptive and vestibular inputs. Arch Ital Biol. 1995; 133:31–45. [PubMed: 7748060]

Precht W, Volkind R, Blanks RH. Functional organization of the vestibular input to the anterior and posterior cerebellar vermis of cat. Exp Brain Res. 1977; 27:143–160. [PubMed: 65291]

Ramsay, JO.; Silverman, BW. Functional data analysis. 2nd edn. New York: Springer; 2005.

Shenoy KV, Sahani M, Churchland MM. Cortical control of arm movements: a dynamical systems perspective. Annu Rev Neurosci. 2013; 36:337–359. [PubMed: 23725001]

Shik ML, Orlovsky GN. Neurophysiology of locomotor automatism. Physiol Rev. 1976; 56:465–501. [PubMed: 778867]

Smith SS. Sensorimotor-correlated discharge recorded from ensembles of cerebellar Purkinje cells varies across the estrous cycle of the rat. J Neurophysiol. 1995; 74:1095–1108. [PubMed: 7500135]

Snyder RL, Faull RL, Mehler WR. A comparative study of the neurons of origin of the spinocerebellar afferents in the rat, cat and squirrel monkey based on the retrograde transport of horseradish peroxidase. The Journal of comparative neurology. 1978; 181:833–852. [PubMed: 99460]

Thomson DB, Isu N, Wilson VJ. Responses of neurons of the cat central cervical nucleus to natural neck and vestibular stimulation. J Neurophysiol. 1996; 76:2786–2789. [PubMed: 8899645]

Todorov E, Jordan MI. Optimal feedback control as a theory of motor coordination. Nat Neurosci. 2002; 5:1226–1235. [PubMed: 12404008]

Tolbert DL, Gutting JC. Quantitative analysis of cuneocerebellar projections in rats: differential topography in the anterior and posterior lobes. Neuroscience. 1997; 80:359–371. [PubMed: 9284340]

Tolias AS, Ecker AS, Siapas AG, Hoenselaar A, Keliris GA, Logothetis NK. Recording chronically from the same neurons in awake, behaving primates. J Neurophysiol. 2007; 98:3780–3790. [PubMed: 17942615]

Udo M, Matsukawa K, Kamei H. Simple and Complex Spike Activities of Purkinje Cells During Locomotion in the Cerebellar Vermal Zones of Decerebrate Cats. Exp Brain Res. 1981; 41:292–300. [PubMed: 7215490]

Vinueza Veloz MF, Zhou K, Bosman LW, Potters JW, Negrello M, Seepers RM, Strydis C, Koekkoek SK, De Zeeuw CI. Cerebellar control of gait and interlimb coordination. Brain structure & function. 2014

Author Manuscript Author Manuscript Author Manuscript Author Manuscript

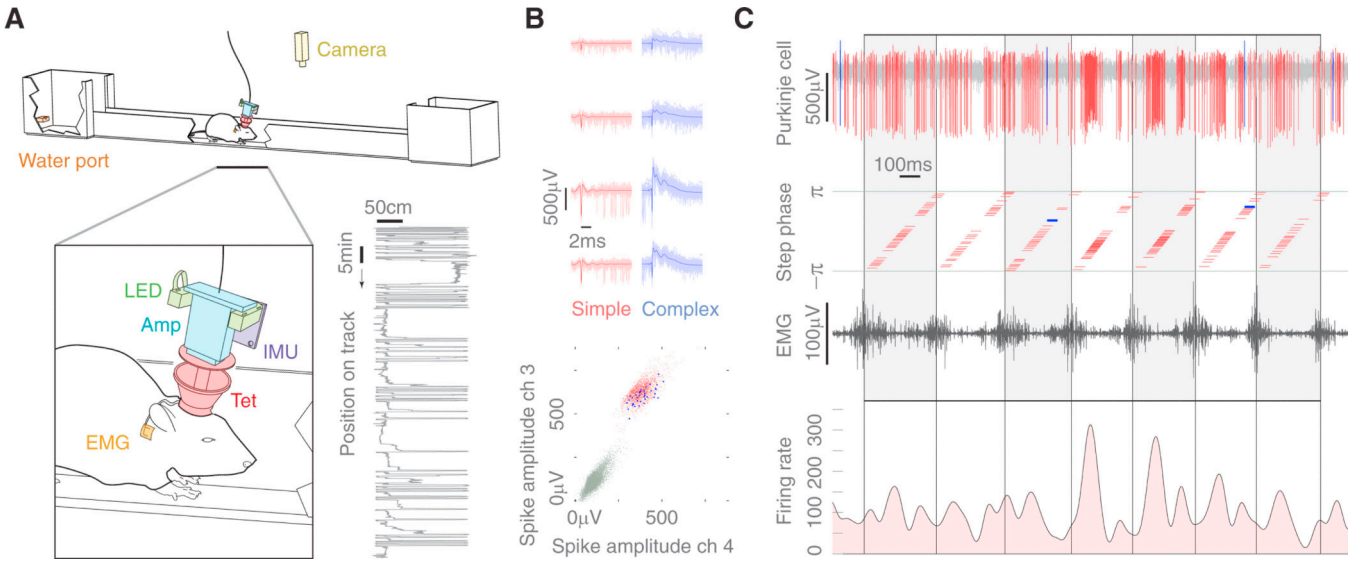

Figure 1. Tetrode recordings from Purkinje cells during locomotion in freely moving rats

(A) Experimental setup. Rats were trained to walk for water reward on a 1.8m long track (see Figure S1). Animal position was measured using an overhead camera and an LED bracket fixed to the headstage (LED). Head pitch and roll were monitored using an inertial measurement unit (IMU), and the stepping rhythm was detected using an electromyogram from the acromiotrapezius (EMG). Purkinje cell activity was recorded using a multi-tetrode array (TET) and headstage-mounted preamplifier (AMP). Behavior in a typical session is shown in the lower right: the animal's position (x-axis) is plotted as a function of time (y-axis). **(B)** Tetrode recording from a Purkinje cell. Simple (red) and complex spike (blue) waveforms for all four channels, as well as spike amplitudes on a pair of channels, are shown. Simple and complex spike firing rates depended on behavioral state (**see** Figure S4). **(C)** Raw data from a single tetrode, along with step phases at spike times and EMG trace (black). The EMG peaks correspond to a step phase of π. The firing rate of the Purkinje cell is shown in the bottom panel. Within each step cycle, the firing rate changes with step phase, but the shape and magnitude of these changes vary extensively across steps.

Author Manuscript
Author Manuscript
Author Manuscript
Author Manuscript

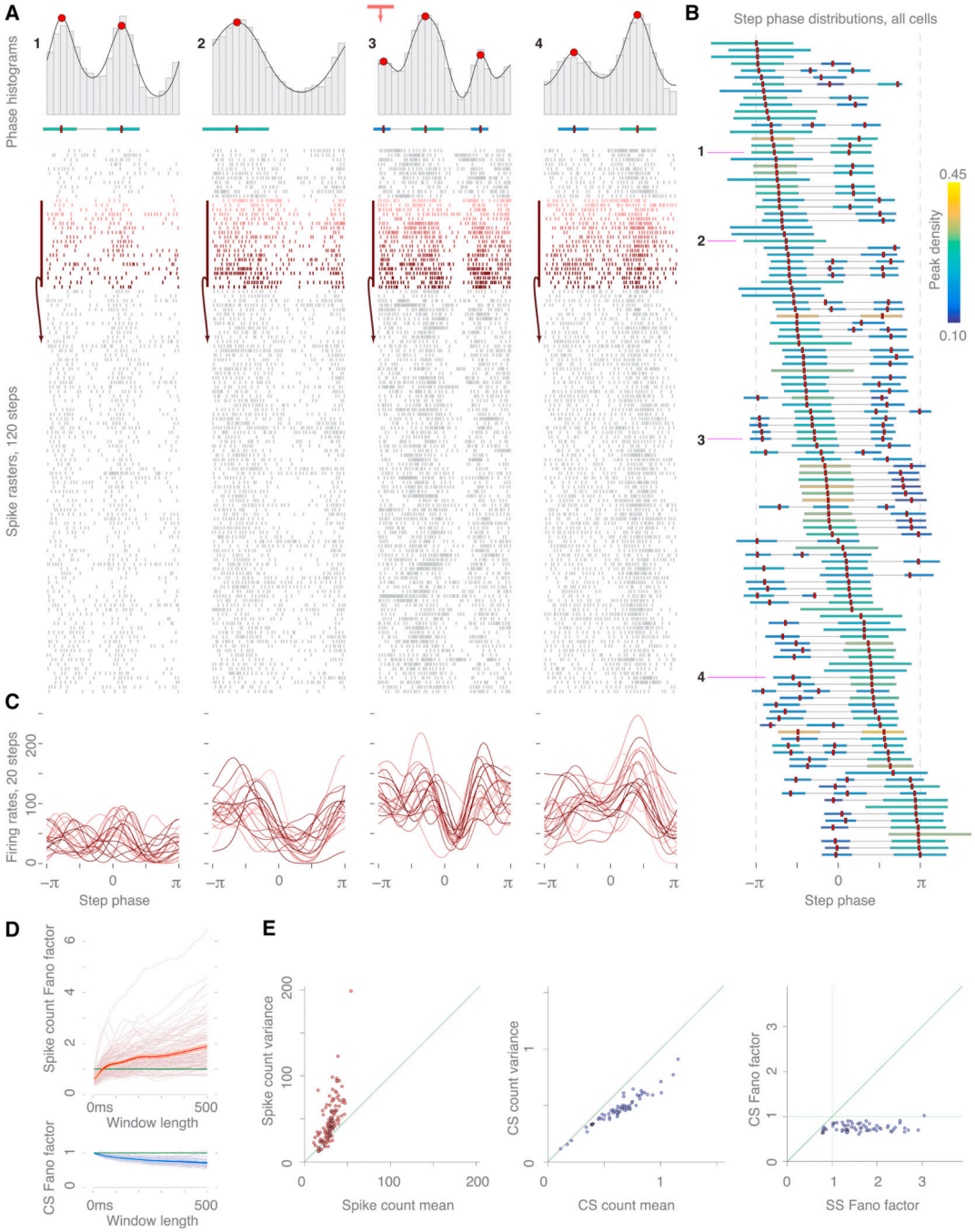

Figure 2. Purkinje cell activity is rhythmically modulated during locomotion, but highly variable across steps

(A) Above, histograms of the step phase at spike times and density fits for four neurons. The example cell from Figure 1 is marked with a red arrow. Below, step-locked spike rasters for the first 120 steps from each dataset. Darker colors represent later cycles. **(B)** All recorded Purkinje cells were significantly tuned to the stepping rhythm, but the number, location, and height of the modes were diverse. Each red marker corresponds to one mode, and the horizontal extent of each bar corresponds to half the distance between the mode and the

Author Manuscript Author Manuscript Author Manuscript Author Manuscript

nearest trough. The scale bar shows the height of the density peaks, encoded as pseudocolor hue. **(C)** Step-locked firing curves for twenty consecutive steps, colored as in **(A)**. These curves exhibit a high degree of variability, which is not evident in the averaged data. **(D)** Variance-to-mean ratios (Fano factors) for step-locked spike counts (above) and complex spikes (below). Each curve represents the Fano factor for a single cell, as a function of the length of the window starting at the EMG peak. Bold lines represent the averages across cells, +/− SEM. The solid green lines show the Fano factor expected for a Poisson process, which is identically one. **(E)** From left to right: spike count variance versus mean, complex spike variance versus mean, and complex versus simple spike Fano factor for a 350ms window. These data indicate that simple spikes are significantly over-dispersed relative to a Poisson process, while complex spikes are under-dispersed.

Author Manuscript Author Manuscript Author Manuscript Author Manuscript

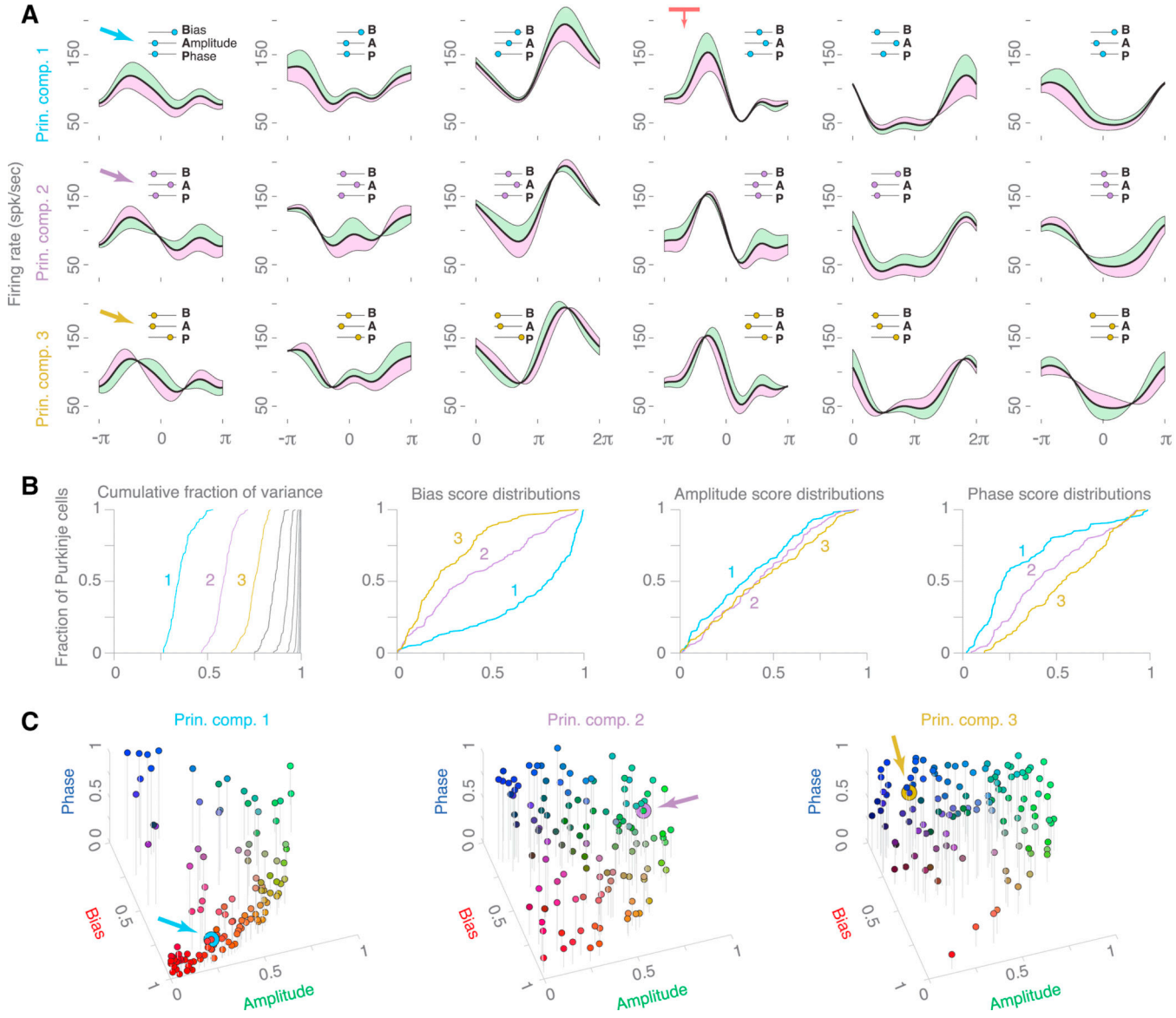

Figure 3. Patterns of step-to-step variability

(A) Mean firing rate curves (black) for six Purkinje cells (columns). Each row shows the effect of adding or subtracting one of the first three principal components for each cell (see also Figure S5). For a mean firing rate curve f(θ) and a principal component coefficient vector w(θ), the green curve shows f(θ) + c*w(θ), and the magenta curve shows f(θ) - c*w(θ), where c = 100 is a constant. In many cases, the components impose a shift in bias, amplitude, or phase. In each panel, the three inset scales show (1) bias score, S_{bias}, (2) amplitude score, S_{amp}, and (3) phase score, S_{phase}. The example cell from figures 1 and 2 (fourth column) is marked with a red arrow. **(B)** Distribution of curve properties across the Purkinje cell population. The left panel shows the cumulative fraction of curve variance due to the first (blue), second (lavender), third (yellow), and fourth through tenth (gray) principal components. The three panels on the right show the distribution of bias, amplitude, and phase scores for each of the first three components. **(C)** Joint distribution of bias, amplitude,

Author Manuscript Author Manuscript Author Manuscript Author Manuscript

and phase scores. In the left panel, the location and RBG value of each point represent (S_{bias}, S_{amp}, S_{phase}) for the first principal component of a single Purkinje cell. For example, the cell marked with the blue arrow is the cell in the first column in **(A)**, and the location of this point corresponds to the bias, amplitude, and phase values on the inset scale in the first row and first column of **(A)**. This cell exhibits a high bias value, but low amplitude and phase values. Similarly, the center and right panels show (S_{bias}, S_{amp}, S_{phase}) for the second and third components, respectively. For many cells, the first component (left panel) is close to a pure bias shift: (S_{bias}, S_{amp}, S_{phase}) ≈ (1, 0, 0) (red points). By contrast, the third component (right panel) often reflects a phase shift: (S_{bias}, S_{amp}, S_{phase}) ≈ (0, 0, 1) (blue points).

Author Manuscript Author Manuscript Author Manuscript Author Manuscript

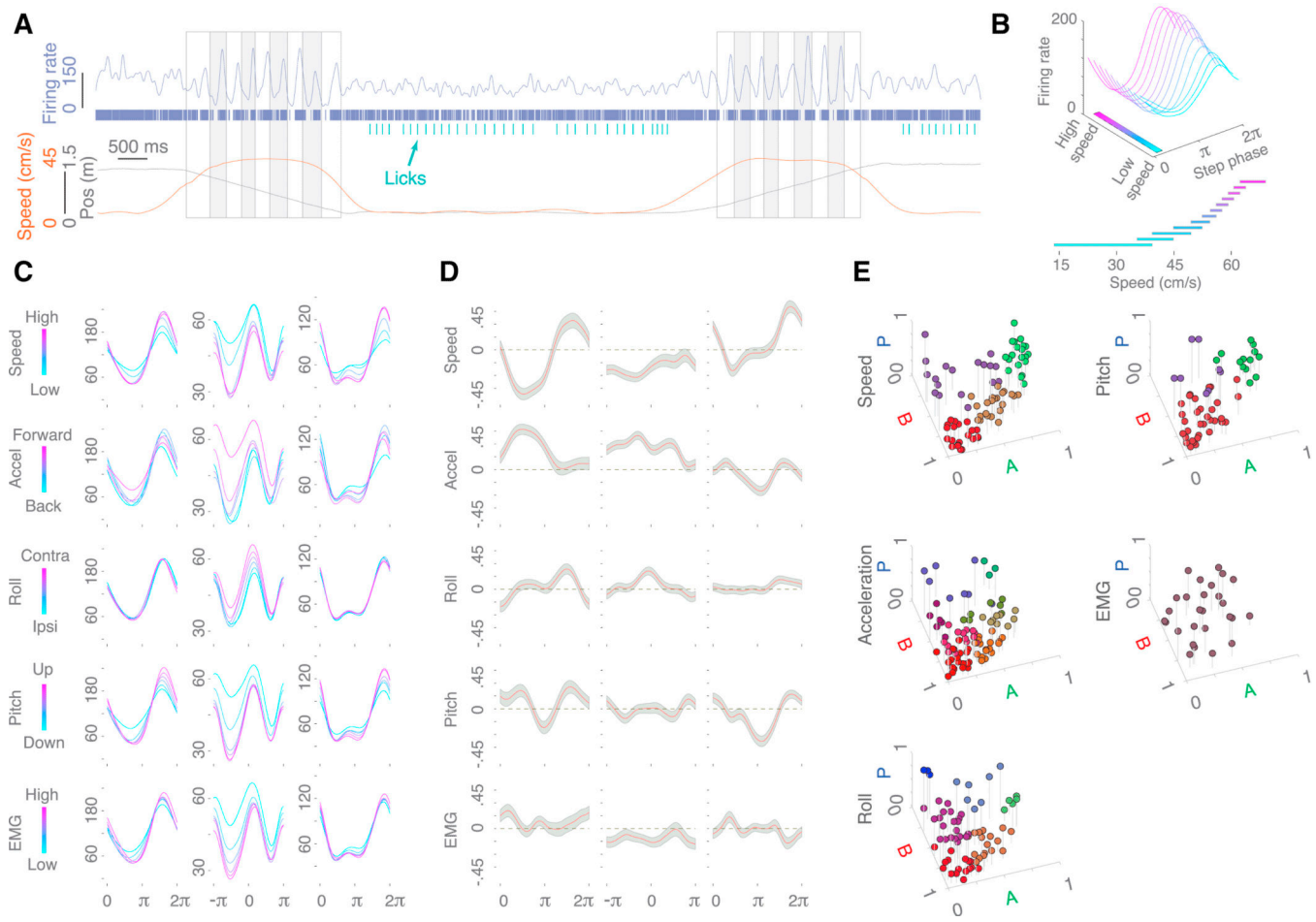

Figure 4. Behavior modulates step-to-step variability in a step-phase-dependent way, revealing functional clusters of Purkinje cells

(A) Spike train and firing rate for a Purkinje cell over two laps, along with the animal's position and speed, and step and lick times. **(B)** Above: wireframe plot showing the dependence of firing rate on animal speed for the cell in **(A)**. Each curve is the average firing rate for steps on which the animal's speed falls within the specified slicing interval. Note the smooth transition from a low-amplitude to high-amplitude curve with increasing speed. Below: slicing intervals used in upper panel. Twelve slicing intervals are used, with 50% overlap. **(C)** Speed-, acceleration-, roll-, pitch-, and EMG-dependent firing rates for three example cells. Six slicing intervals are used, with 50% overlap. The neuron from **(A)** and **(B)** is shown in the left column. The regression coefficients for the step-averaged firing rates are shown in Figure S6. **(D)** Phase-dependent regression curves for the cells in **(C)**. Bands show 95% confidence intervals. Behavior has a strong, phase-dependent effect on firing rates for many cells, which varies across different behavioral variables. **(E)** Bias, amplitude, and phase analysis of regression curves reveals functional clustering of Purkinje cells. For each behavioral variable, the 3D scatterplot shows (S_{bias}, S_{amp}, S_{phase}) values of the regression curves for cells significantly modulated by that variable. Points are colored using RGB values of the cluster averages of (S_{bias}, S_{amp}, S_{phase}). Note a concentration of points around (S_{bias}, S_{amp}, S_{phase}) = (1, 0, 0) (bias shifts) for all behavioral variables except

Author Manuscript Author Manuscript Author Manuscript Author Manuscript

EMG amplitude, around (S_{bias}, S_{amp}, S_{phase}) = (0, 1, 0) (amplitude shifts) for speed and pitch, and around (S_{bias}, S_{amp}, S_{phase}) = (0, 0, 1) (phase shifts) for acceleration and roll.

Author Manuscript Author Manuscript Author Manuscript Author Manuscript

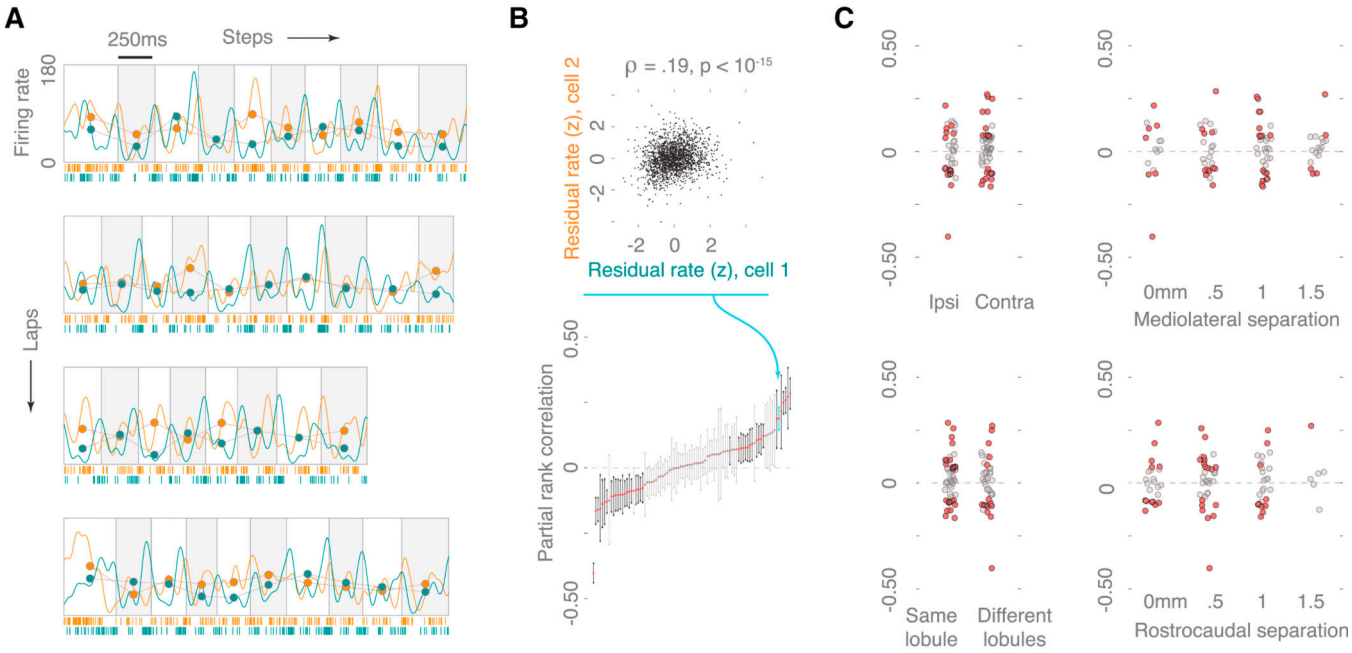

Figure 5. Step-to-step variability is correlated across Purkinje cells

(A) Stepping sequences on four consecutive laps, along with spike trains and firing rates for a pair of simultaneously-recorded neurons (orange and teal). The step-averaged firing rates, shown as dots, often suggested coordinated changes between pairs. **(B)** Above: a scatterplot of residual firing rates for the pair of cells in **(A)** reveals that the step-averaged firing rates were correlated after removing the effects of behavioral factors. These correlations were not due to nonlinear interactions between measured behavioral variables and firing rates (Figure S7). Below: the partial rank correlations (Spearman's ρ for the regression residuals) between firing rates for pairs of cells (z-scores) are shown with 95% confidence intervals (above). Many pairs are significantly correlated (q = .05, bold), both positively and negatively. **(C)** Pairwise correlations do not depend on the relative anatomical location of the recorded cells. Panels show the distribution of correlation values for pairs on the same and opposite sides of the brain, in the same or different lobules, and as a function of mediolateral and rostrocaudal separation. Correlation values significantly different from zero are plotted in red.

Author Manuscript
Author Manuscript
Author Manuscript
Author Manuscript

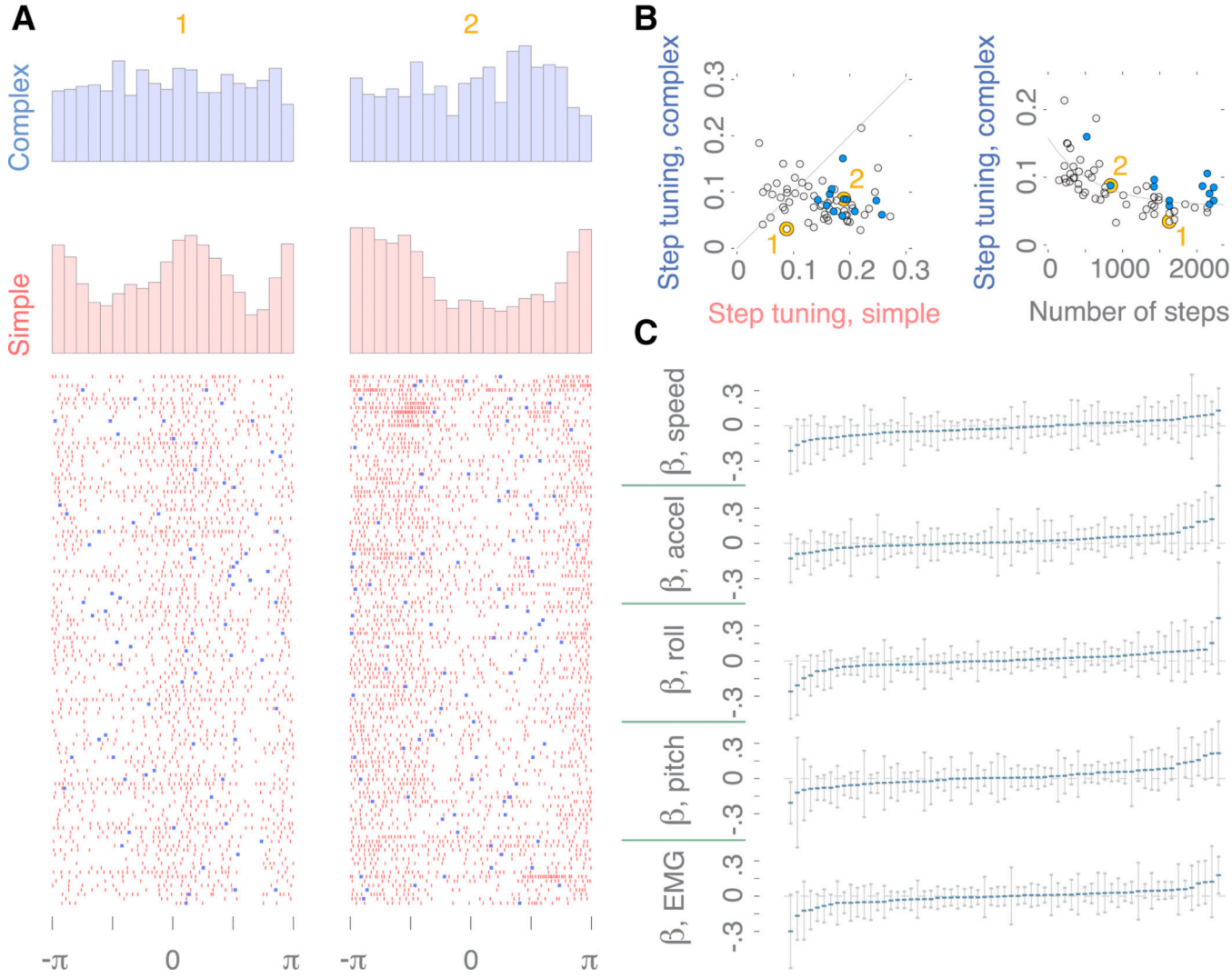

Figure 6. Complex spikes show modest tuning to step phase, but are not related to behavioral variables across steps

(A) Simple spike (red) and complex spike (blue) step phase histograms for the two example Purkinje cells highlighted in orange, along with the spike rasters for the first 120 steps. Cell 2 showed statistically significant complex spike tuning. **(B)** Left: step tuning strength (Kuiper's statistic; see Methods) for simple and complex spikes. Cells with significant complex spike tuning are plotted in blue. Simple spike tuning was significant for all recorded cells. Right: complex spike step tuning strength against the number of steps in the dataset. Some of the largest values of step tuning strength likely result from a small number of observed step cycles. **(C)** Linear model coefficients for behavioral predictors of complex spikes, with 95% confidence intervals. Complex spikes are not significantly modulated by speed, acceleration, head posture, or EMG amplitude for any cells. These results suggest that the parallel and climbing fiber systems convey distinct types of information during locomotion.

Author Manuscript Author Manuscript Author Manuscript Author Manuscript

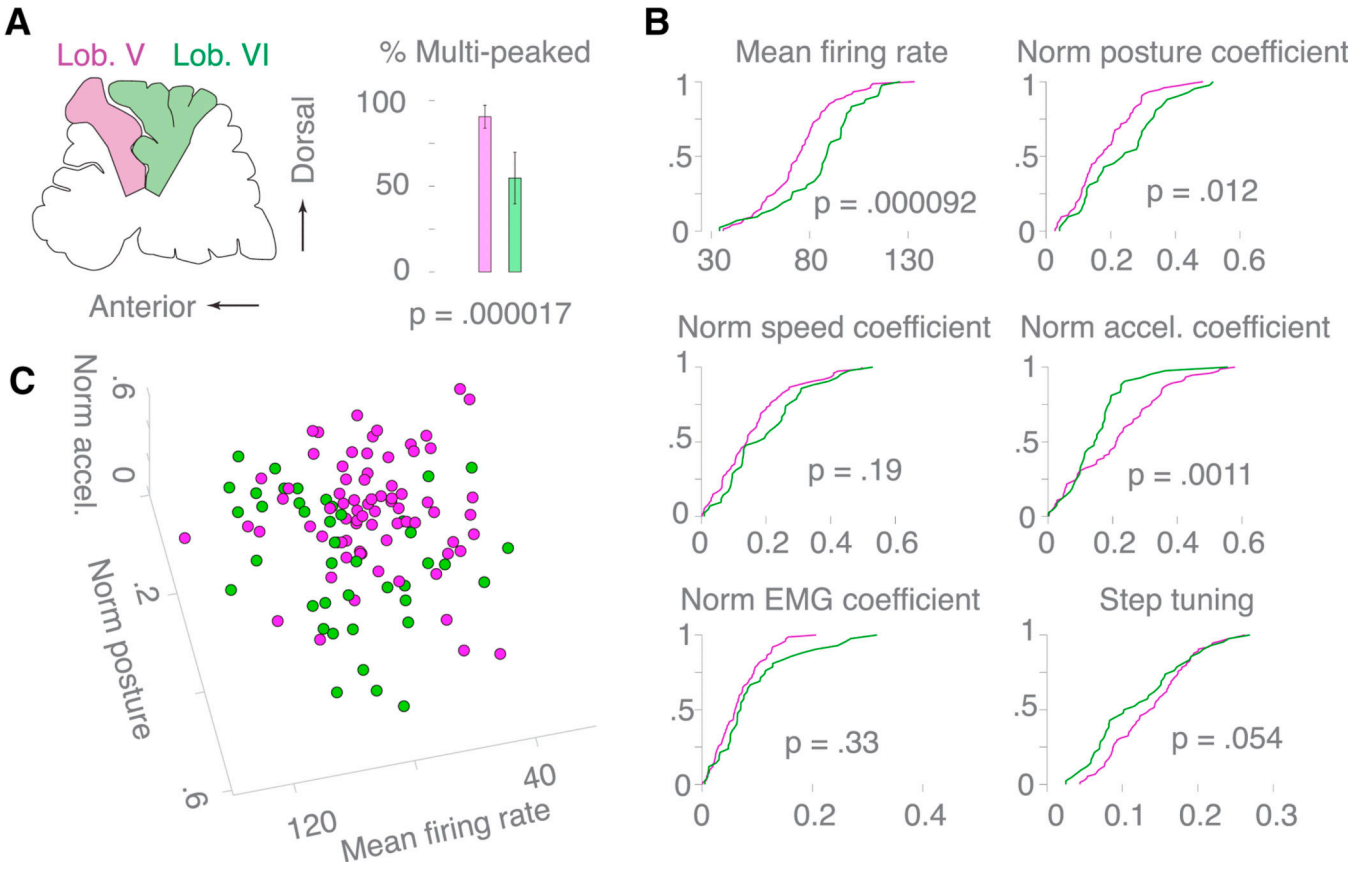

Figure 7. Purkinje cell properties differ across cerebellar lobules V and VI

(A) Left: sagittal view of the cerebellum, highlighting lobules V (magenta) and VI (green). Right: percentage of cells in each lobule with more than one activity peak in the step cycle. 91% of lobule V Purkinje cells have multiple peaks in the step cycle, in comparison with only 55% in lobule VI. **(B)** Distribution of mean firing rates, step tuning (Kuiper's statistic), and the norms of the head posture coefficients ($\sqrt{(\beta_{roll}^2 + \beta_{pitch}^2)}$), speed coefficients ($|\beta_{speed}|$), acceleration coefficients ($|\beta_{acc}|$), and EMG coefficients ($|\beta_{EMG}|$), for Purkinje cells in lobules V and VI. Cells in lobule VI have higher firing rates, are more modulated by head posture, and are less modulated by acceleration than lobule V cells. **(C)** Joint distribution of firing rates, the norm of the acceleration coefficients, and the norm of the posture coefficients. These differences are consistent with a larger role for lobule V in limb control during locomotion, and for lobule VI in the control of the neck and head.

Author Manuscript Author Manuscript Author Manuscript Author Manuscript

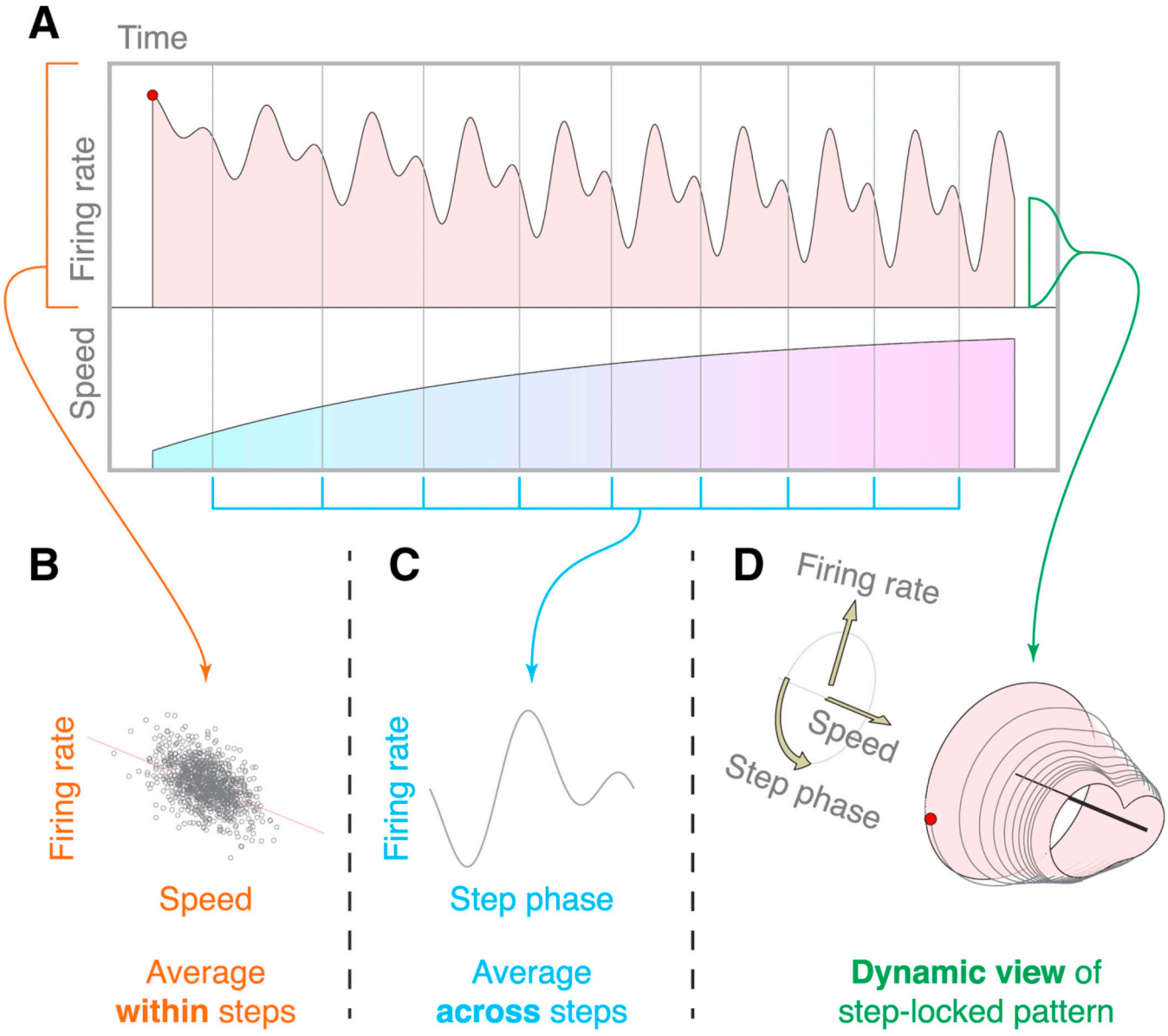

Figure 8. A dynamic view of neuronal activity during locomotion

(A) A schematic Purkinje cell with a step-locked pattern controlled by a single parameter, speed. Note the systematic transition in the firing rate curve as speed increases; c.f. experimental data in Figure 4B, C. **(B)** A view of the activity of the schematic neuron in **(A)** after averaging within steps. A relationship between speed and firing rate is apparent, but the dependence of activity on step phase within each cycle is obscured. **(C)** A view of the same neuron's activity after averaging across steps. While this view reveals the dependence of firing rate on step phase, it obscures step-to-step variability and its dependence on speed. **(D)** A dynamic view of the cell's step-locked firing pattern. Each step produces one full rotation around the speed axis, and as the animal's speed increases, the firing rate follows the trajectory from **(A)**, shown in gray. Under this view, the step-locked firing pattern is

itself shaped by behavioral factors during locomotion, allowing flexible control of movement under dynamic conditions.

Author Manuscript Author Manuscript Author Manuscript Author Manuscript